Routes to Rubber Nanocomposites

*Amit Das, Klaus Werner Stöckelhuber, Rene Jurk, Gert Heinrich**

Summary: This paper presents recent developments in rubber nanocomposites from the laboratory of the authors. In particular, the preparation of rubber nanocomposites with improved performance from layered silicates, carbon nanotubes and *in situ* sol-gel derived silica nanoparticles incorporated in different elastomers and by different methods for the development of rubber nanocomposites with improved performance is described.

Keywords: CNT; *in situ* sol-gel silica; layered silicate; nanocomposite; rubber

Introduction

Although carbon black is still considered one of the most important reinforcing agents in rubber technology, precipitated silica – in conjunction with a suitable coupling agent – shows the tendency to become a dominant filler material especially in tire technology for passenger car tire tread applications. The growing interest for silica technology was caused by increasing demands for economic fuel consumption and improved safety on wet and icy roads imposed on the tire production technology.

Furthermore, in the last decade the use of new sub-micron particles as fillers in a polymer matrix has gained considerable attention for tire and also for non-tire rubber applications. The exploitation of the large surface areas of these fillers is the main reason for the enhancement of the performance of the corresponding polymer (elastomer) composites. For this purpose, the nanoparticles, considered for the preparation of rubber nanocomposites, include layered silicates,[1–5] layered double-hydroxides,[6–7] nanosilica,[8–9] expanded graphites,[10–11] and carbon nanotubes.[12–13]

In situ sol-gel generated silica particles have proved to be an excellent material for the synthesis of hybrid organic-inorganic systems where the organic and inorganic component are mixed on the molecular level.[14]

Owing to the delamination property of layered silicate, extensive efforts are made to prepare rubber nanocomposites with layered silicates. A very low loading of exfoliated layered silicates very often delivers significantly-enhanced mechanical properties to the nanocomposite as compared to unfilled polymers.[15–18]

The dimensions of carbon nanotubes (CNTs) are from a few microns up to millimeters in length, and several nanometers in diameter. A single nanotube is approximately one hundred times stronger and six times lighter than steel, and it exhibits good electrical and thermal conductivity. Tremendous attention is now paid from all over the world to the use of carbon nanotubes as electrically conducting and reinforcing fillers for polymers.[19–21] However, it is very difficult to disperse CNT in polymers because they produce highly entangled agglomerates like felted threads.

In the main body of this chapter, we present some recent developments in rubber nanocomposites. In particular, we describe new results from our work where layered silicates, carbon nanotubes and *in situ* sol-gel derived silica nanoparticles are incorporated in different elastomers by different methods to develop rubber nanocomposites with improved performance.

Leibniz-Institute for Polymer Research, Dresden, D-01069, Germany
Fax: +49 (0)351 4658 362; E-mail: gheinrich@ipfdd.de

Experimental Part

S-SBR-Nanocomposites Using Layered Silicates

For the preparation of rubber nanocomposites based on solution-polymerized styrene-butadiene rubber (S-SBR) with layered silicates, we developed a masterbatch technology using a polar rubber: carboxylated nitrile butadiene rubber (XNBR) as a dispersing agent for the layered silicate.[15] Filled rubber blends of S-SBR and butadiene rubber (BR) are widely used in tire technology for several passenger car tire tread applications. In our case, the S-SBR-layered silicate rubber composites were prepared by a two-step method. In the first step, organomodified clay was mixed with XNBR in an internal mixer (HAAKE PolyLab-System, Thermo Electron, Karlsruhe, Germany) at 160 °C with a rotor speed of 50 rpm during 10 min. In the second step, this obtained masterbatch was mixed with S-SBR in an open two-roll mixing mill (Polymix 110L, size: 203 mm × 102 mm Servitech GmbH, Wustermark, Germany), and, subsequently, additives such as zinc oxide, stearic acid, organic accelerators and sulfur were added.

NBR-Nanocomposites Using Layered Silicates

Acrylonitrile butadiene rubber (NBR) is commonly considered the workhorse of several industrial and (non-tire) automotive rubber products. The compounding of NBR with organoclay and vulcanization ingredients was done by a laboratory-size open two-roll mixing mill and by an internal mixer in dependence of the mixing temperature. Finally, the accelerator, sulfur and ZnO were added to the mix within 5 min.[16]

EPDM-Nanocomposites Based on in Situ Sol-Gel Generated Silica Particles

Ethylene-propylene-diene-monomer (EPDM) rubbers are characterized by a wide range of industrial applications. The main properties of EPDM are its outstanding heat, ozone and weather resistance. Reinforcing nanosilica particles in EPDM rubbers are prepared by an *in situ* sol-gel method.[14] In this method, EPDM was mixed with 4 g bis(3-triethoxy silylpropyl)tetrasulfide (TESPT) per 100 g of rubber (4 phr) in an internal mixer at 160 °C, having a rotor speed of 50 rpm for a predetermined time. It was observed from the rheometric study at 160 °C that there is no increment of torque within 15 min time. Therefore, the maximum pre-heating time in the mixer was chosen to be up to 11 min. The material thus obtained was transformed into a thin sheet using an open two-roll mixing mill, followed by subjecting the film to swelling in the tetraethylorthosilicate solution (TEOS) for 72 h. After removal from the TEOS solution, the rubber was dipped into 10% *n*-butyl amine aqueous solution for 24 h to get silica particles by the condensation reaction of TEOS. The obtained sheet was dried for several days at room temperature. Finally, the sheet was again dried in a vacuum oven for 8 h at 70 °C. The silica-filled EPDM rubber was mixed with rubber additives and then vulcanized.

S-SBR-BR Nanocomposites Based on Carbon Nanotubes (CNT)

The CNTs was incorporated in solution-polymerized styrene-butadiene rubber (S-SBR) and butadiene rubber (BR) blend, with a special method.[20] The multiwalled carbon nanotubes were dispersed in ethanol in the ratio 1:10 by weight in the case of unmodified carbon nanotubes. For the hydroxyl-modified carbon nanotubes, the nanotube-alcohol ratio was chosen to be 1:30. In each case, 2.5 phr of the non-ionic surfactant was added to the dispersed CNT. This mixture was then treated gently in an ultrasonic bath (200 $W_{effective}$; 25 kHz) for approximately 2 h. The mixture thus obtained was mixed into the rubber. In the first step, 50 g S-SBR and 50 g BR were mixed in an open two-roll mixing mill of laboratory size during 5 min at 80 °C. Then, the ethanolic CNT–suspension was added to the mixture very slowly. The mixing time for the incorporation of the nanotubes was about 15 min. For comparison also rubber composites were produced where the carbon nanotubes were mixed directly (dry) into the rubber compound. Finally,

the curing chemicals were incorporated into the composites at room temperature.

Results and Discussion

Layered Silicate in S-SBR

The contents of each masterbatch is presented in Table 1. From each masterbatch, 5, 10 and 15 g of compounds were taken and were incorporated to 100 g of S-SBR. Figure 1 shows the X-ray diffraction patterns for the rubber compounds of S-SBR with organomodified layered silicate. The 2θ-values along the x-axis can be converted to layer spacing values d by the Bragg relationship ($\lambda = 2d \sin\theta$, where λ is the wavelength of the radiation). A broad peak appears at about 1.32 nm for unmodified clay, whereas this peak is shifted to 2.98 nm for organomodified clay. For S-SBR matrix with 5, 10 and 15 phr of M-60 (masterbatch with 60 phr layered silicate), the corresponding values are 4.43 nm, 4.01 nm, and 3.82 nm, respectively. The diffraction peak of organoclay is shifted towards the low-angle direction, indicating the effective expansion of the interlayer distance of the clay. However, the interlayer spaces decrease with an increase of clay content. Apparently, with increasing filler loading, not enough space is available where the clay layers could occupy their positions without sacrificing the gallery gap.

Table 1.
Preparation of the XNBR master batch.

Master batch	XNBR (g)	Organoclay (g)
M-30	100	30
M-40	100	40
M-50	100	50
M-60	100	60

Transmission electron microscopy delivers a direct visualization of the dispersion of the organoclay in the polymer matrix. Figure 1 also shows the TEM picture of S-SBR where 5 phr M-60 has been used. The actual organoclay concentration of the vulcanizate is 1.8 phr. This figure shows many small dark lines preferentially oriented in a north-south direction. Here, the organoclay is distributed evenly in the whole rubber matrix.

Results of tensile tests are shown in Figures 2a-2d. In Figures 2a and 2b, the stress values at 100% and 300% elongation are plotted against the amount of clay and are compared to the samples without clay, which are plotted against the amount of XNBR. Although the clay is always accompanied by XNBR, we do not display its amount for better understanding. It is evident from these figures that with an increase of the filler amount, the modulus increases with a linear tendency. In contrast, in the unfilled samples containing S-SBR and XNBR, the corresponding physical values are very low. These obser-

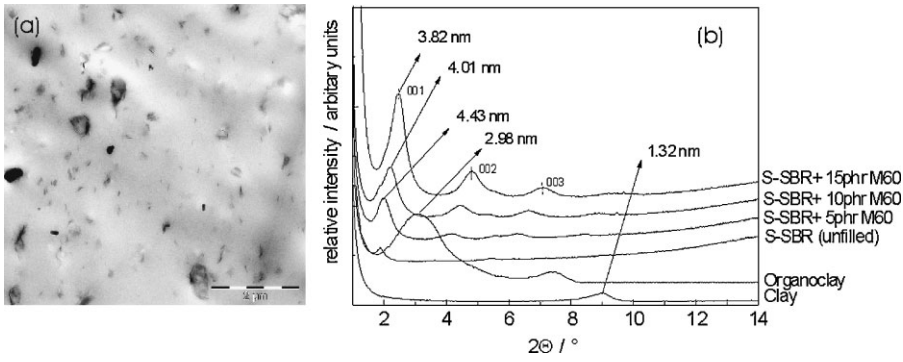

Figure 1.
(a) Transmission electron micrograph of layered silicate-filled S-SBR, (b) XRD spectra of S-SBR reinforced with organically modified montmorillonite. The spectra of the related clays and organoclay are also shown. The position of the (001), (002), and (003) reflexes is indicated by dotted line.

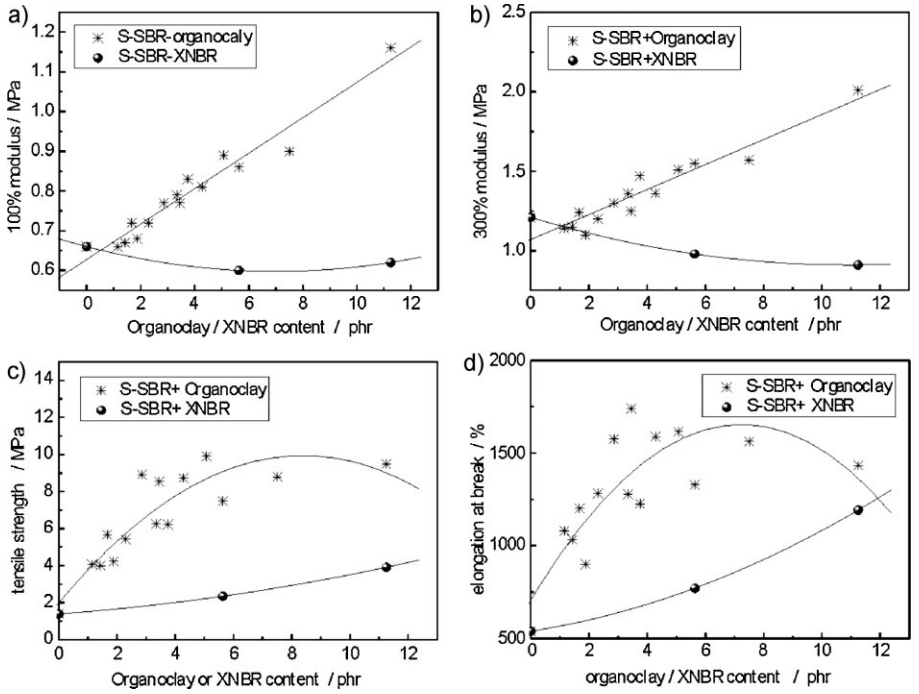

Figure 2.
(a) Dependence of the 100% modulus values on the organoclay and XNBR amount. (b) Dependence of the 300% modulus values on the organoclay and XNBR amount. (c) Dependence of the tensile strength values on organoclay and XNBR amount. (d) Dependence of the elongation at break values on the amount of organoclay and XNBR.

vations prove that the obtained higher rigidity of the rubber matrix is not caused by the XNBR part and support the suggestion of reinforcement caused by the organoclay. Concerning tensile strength, the above-mentioned fact is also reflected in Figure 2c. For the samples with around 5 phr loading, seven times higher values in tensile strength are obtained compared to the gum. It is also found from the polynomial fit curve in Figure 2c that there is a maximum of tensile strength at around 5 to 8 phr organoclay. At higher loading, the clay particles aggregate and consequently do not contribute to the ultimate strength of the composite. In contrast, an equivalent amount of XNBR without any filler deteriorates the corresponding mechanical properties of the composites. Thus, it can be stated that the organomodified layered silicate not only provides excellent reinforcement effects on the rubber matrix, but it also acts as a compatibilizer between polar and non-polar rubber as mentioned before. The investigated types of rubber nanocomposites also show very high elongation at break values as presented in Figure 2d. High elongation at break values are otherwise found in silica-filled rubber compounds with a direct chemical bonding between polymer and silica. In the rubber nanocomposites made of XNBR, S-SBR and organoclay, it can be assumed that the surface silanol groups of the layered silicates react with the carboxyl groups of the XNBR and, therefore, direct rubber-filler bonds are formed. In this way, the high elongation properties can be explained.

Layered Silicate in NBR

Figure 3a shows the X-ray diffraction pattern for sulfur- and peroxide-cured NBR-organoclay nanocomposites, respectively. The X-ray diffraction peaks at $2\theta = 3.06^{\circ}$ represent the diffraction of the (001) crystal surface of the silicate

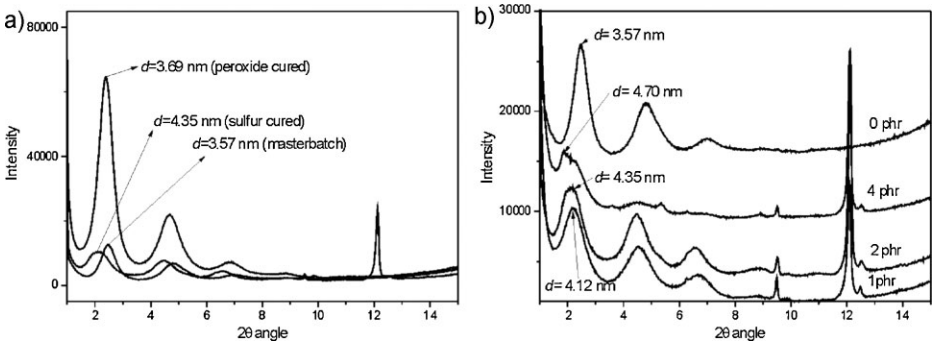

Figure 3.
WADX patterns of NBR reinforced with 5 phr organoclay and cured by (a) sulfur, peroxide and NBR masterbatch; (b) cured by sulfur in the presence of 1, 2 and 4 phr stearic acid and without stearic acid.

particle in the sulfur-cured NBR vulcanizate (Figure 3a), corresponding to a *d*-spacing of 4.35 nm. This indicates that a relatively large gallery expansion in layered silicates has taken place during the melt-mixing and curing at 160 °C. In the case of peroxide-cured systems (Figure 3a), we found the diffraction peak of the (001) crystal surface at 2θ equal to 3.38°, corresponding to a *d*-spacing of 3.69 nm. Here, the gallery gap between two parallel plates of silicate particles has been increased also to a considerable extent. However, the extent of space increment is higher in the case of the sulfur-cured system as compared with the *d*-spacing from the masterbatch (Figure 3a).

The effect of stearic acid on the exfoliation / intercalation process of the layered silicate has also been studied by X-ray diffraction experiments. For this study, different amounts of stearic acid are taken in sulfur-curing packages. Generally, in a sulfur-curing package for diene rubber, 2 phr is the standard dose of stearic acid. For that reason, we have taken 1 to 4 phr stearic acid in our formulation which are below and above the standard dose. Very interesting X-ray diffraction patterns have been recorded for these formulations and the corresponding X-ray diffractograms are given in Figure 3b. The interlayer distances of the silicate particles in the NBR matrix containing 1, 2, and 4 phr stearic acid are 4.12, 4.35 and 4.70 nm, respectively, whereas in the used masterbatch compound the interlayer distance between two adjacent silicate layers is 3.57 nm. This means that the interlayer distance increased during sulfur mixing and/or curing, and an excess amount of stearic acid favors the extent of intercalation. With an increase in the stearic acid content, the corresponding scattered X-ray peak from the (001) crystal face of silicate particles shifts toward lower angles with a higher space gap. Ultimately, at 4 phr stearic acid content, the diffraction curves show almost exfoliated type scattering pattern at higher order reflections such as (002) and (003), with a very small number of intercalated structures. As a conclusion, a higher amount of stearic acid is recommended for the preparation of rubber-layered silicate nanocomposites. Very recently, Ma *et al.*[22] also reported that stearic acid increases the gallery gap. However, they did not find any change in the gallery gap after adding the stearic acid-treated organoclay into the rubber matrix. The space gap between two clay layers was confined to 3.9 nm.

To observe the effect of multifunctional rubber additives, the zinc salt of dithiophosphate (ZDP) has been used in the curing packages in place of the conventional zinc salt of dithiocarbamate (ZDMC). A shift of the intensity peak in X-ray diffraction to lower diffraction angles indicates that intercalation is a common phenomenon in these systems and that ZDP cured vulca-

nizates show a higher gallery gap between two successive layers of silicate particles (Figure 4a). They also showed a significant reduction of peak intensity of the (002) and (003) crystal faces with a peak broadening effect which signifies the uneven and irregular fashion of intercalation. Ultimately, it can be assumed that ZDP enhances the intercalation process of the layered silicate. This substance, being a multifunctional rubber additive, plays a special role as compatibilizer between organic polymers and inorganic silicates by providing an extra interaction as proposed in Scheme 4b. It explains how ZDP is grafted onto the surface of clay layers, and how this compound acts as a sulfur cross-linking precursor to the rubber chains bringing out some sort of compatibility between the clay and the rubber. It is also noteworthy to mention that all sulfur-cured gum compounds containing ZDMC are showing one sharp peak around $d = 0.72$ nm. It is easily understandable that this scattering comes from sulfur vulcanization ingredients or from the *in situ* formation of some crystalline product from those sulfur curatives. Pure peroxide cured rubber and the masterbatch compound did not show any scattering in this area since it did not contain any other crystalline substances.

Figure 5a and Figure 5b present TEM images of the nanometer-sized layered silicate in the sulfur- and peroxide-cured NBR matrix, respectively. In both cases, the exfoliated layered silicate can be observed. However, some silicate particles in intercalated form are also present. Actually, it is quite a common situation

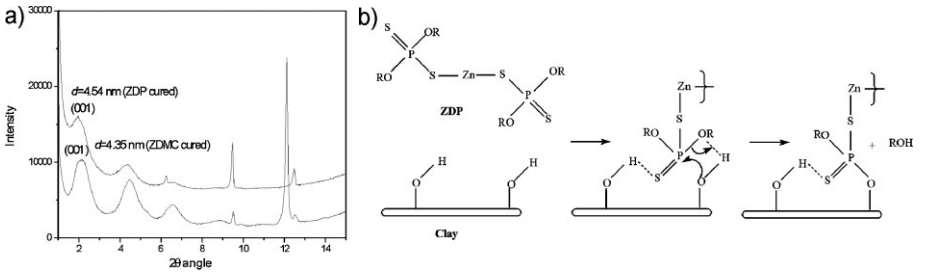

Figure 4.
(a) WAXD patterns of zinc dithiocarbamate (ZDMC) and zinc dithiophosphate (ZDP) cured layered silicate filled NBR, and, (b) probable chemical interaction between ZDP and the silanol groups of the layered silicate surface.

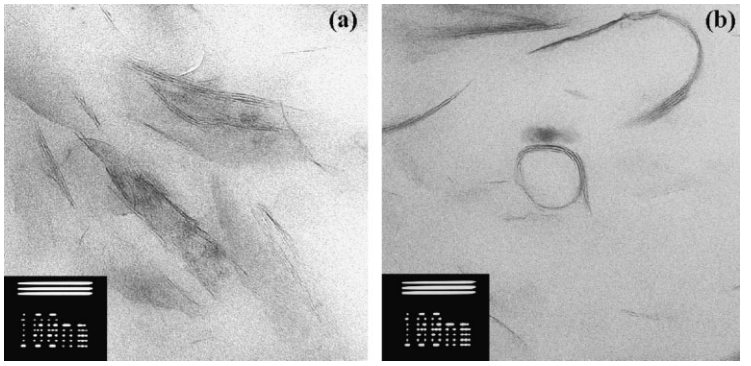

Figure 5.
Transmission electron micrographs of NBR-layered silicate nanocomposite cured using (a) sulfur and (b) peroxide.

to get a bimodal rubber matrix type, consisting of both exfoliated and intercalated silicate layers rather than purely exfoliated.

In Situ Sol-Gel Nanosilica in EPDM

Table 2 shows the method of preparation of the silica-EPDM nanocomposite and the amount of silica generated in the EPDM rubber matrix. The stress-strain diagrams observed for EPDM vulcanizates are plotted in Figure 6. This figure shows that the maximum tensile properties are achieved for the vulcanizate produced by a preheating procedure (in the course of 11-minute heating) in the presence of the silane coupling agent. The corresponding gum vulcanizate shows inferior tensile properties.

It is interesting to note that sol-gel vulcanizates are always stiffer and they have a larger tensile strength, as compared to the conventional filled system EPDM-VN3. This is because the silica particles derived from the sol-gel process provide a stronger reinforcement compared to the conventional silica-filled vulcanizates. The shapes of the curves describing the stress-strain relations for the gum (EPDM) and vulcanizates filled with 4.7 phr commercial silica (EPDM-VN3) are the same for the values of elongation that are less than that corresponding to 50% extension of the initial rubber sample. For larger elongations, the stress observed for the silica-filled composite is greater than that found for its unfilled counterpart measured at the same value of elongation. At the same time, the maximal elongation is found to be higher for the unfilled gum than for vulcanizates filled with 4.7 phr silica. Thus, we may conclude that 4.7 phr silica, conventionally blended in EPDM rubber, shows no, or only marginal, reinforcing activity. In contrast to this observation, a sample filled with 4.7 phr silica grown *in situ* at TESPT grafted EPDM shows a pronounced reinforcement effect (Figure 6a). In this case, the shape of the stress-strain curve is steeper as compared to that observed for the conventional sample and leads to higher maximum stress. Even such a small amount of silica fillers grown *in situ* by the sol-gel method as 5 phr or less can provide considerable reinforcement of the EPDM rubber.

The TEM observation (Figure 6b and 6c) supports the above discussion that in the presence of grafted alkoxysilyl groups the silica particles are grown as more or less mono-dispersed spheres, similar to that of primary particles (Figure 6b, EPDM-TESPT-11-SG). In the presence of TESPT in the rubber matrix (in the absence of heat treatment), the amount of silica is higher, but the size distribution of the particles is more polydisperse, and some of the particles form primary particle agglomerates (Figure 6c: EPDM-TESPT-SG). Furthermore, Figure 6d shows a very small number of silica particles for EPDM-SG where no TESPT has been used before applying the sol-gel process. This clearly indicates that in

Table 2.
Preparation and curing characteristics of the EPDM rubber compound.

Sample code*	Method	Amount of silica (g)
EPDM	Gum, without filler	0
EPDM-TESPT-6-SG**	6 min heating at 160 °C with TESPT	6.3
EPDM-TESPT-11-SG	11 min heating 160 °C with TESPT	4.75
EPDM-TESPT-SG	Room temperature mixing with TESPT in two-roll mill	12.65
EPDM-SG	Only milling in two-roll mill	4.46
EPDM-VN3***	Silica in two-roll mill	4.75

*For each mix 2 phr (per hundred gram of rubber) stearic acid, 5 phr zinc oxide, 4 phr SDT 50 (organic accelerator) and 0.5 phr sulfur were mixed as curatives before the vulcanization process.
**SG signifies processed with the sol-gel technique.
***4.75 phr Ultrasil VN 3 (commercial precipitated silica) was mixed by mechanical mixing to compare with EPDM-TESPT-11-SG.

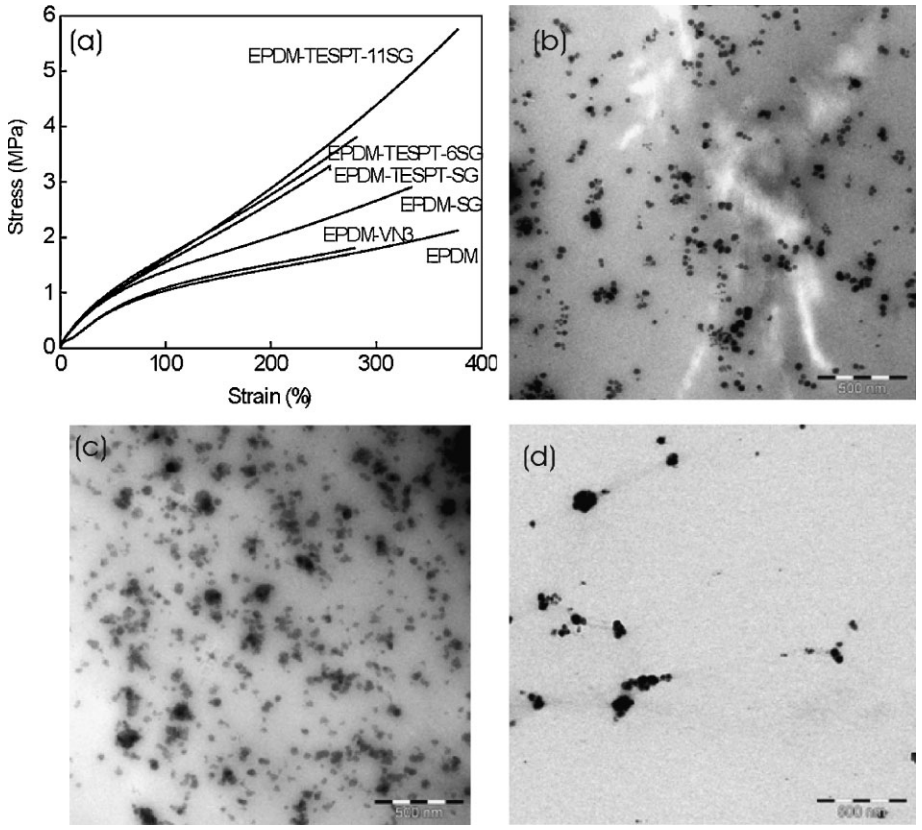

Figure 6.
(a) Tensile stress-strain plot of silica filled EPDM vulcanizates, transmission electron micrographs of the sol-gel derived silica in the EPDM matrix (b) EPDM-TESPT-11SG, (c) EPDM-TESPT-SG and (d) EPDM-SG.

EPDM rubber the presence of TESPT plays a crucial role in the formation of silica particle from TEOS.

Multiwalled Carbon Nanotubes in S-SBR-BR Blend

The structure of CNTs and the state of their dispersion in the S-SBR-BR blend (mixed in the wet method by ethanolic dispersion) were visualized using transmission electron microscopy. Figure 7a reveals that the carbon nanotubes form percolated networks at 5 phr loading.

The storage modulus of unfilled rubbers, E', depends on frequency and temperature, and is independent of the deformation amplitude. In contrast, E' for the filled rubber shows a significant dependency on the dynamic deformation,[23] with the value here considerably decreasing with an increasing strain amplitude.

This non-linear behavior of filled rubbers is known as the 'Payne effect'[23] and has been explained by the existence of a filler network in the rubber matrix above the percolation threshold. With increasing strain amplitude, the filler network is breaking down which results in a lowering of the dynamic storage modulus E'. Figure 7 provides evidence for the existence of a carbon nanotube filler network in a S-SBR-BR blend prepared by the wet mixing method. For a pure rubber (not shown here) and at small CNT loading (up to 2 phr), no 'Payne effect' is observed. However, with the increase of the CNT content a gradual decrease in E' is observed in strain sweeps. Thus, even with 3 phr of

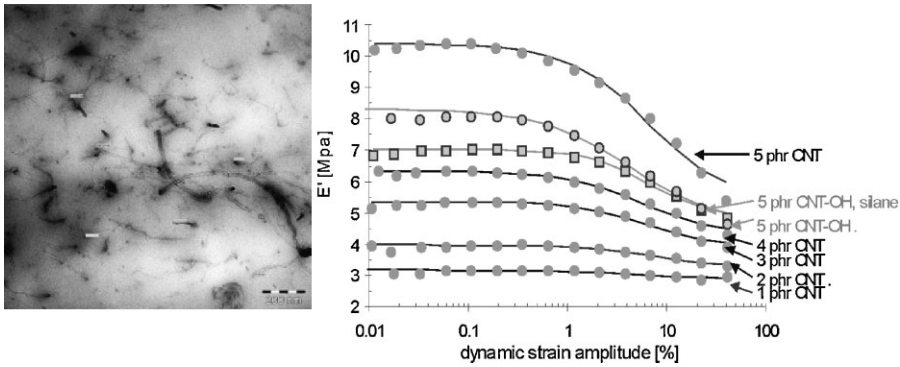

Figure 7.
(a) Transmission electron micrograph of CNT-filled (5 phr) SSBR-BR blends produced by the wet method, and, (b) strain dependencies of dynamic properties for CNT-filled SSBR-BR blends.

CNT, the tubes form a continuous filler network in the rubber matrix. The OH-functionalized sample with 5 phr of CNT shows a significantly lower E' value compared to the unfunctionalized one, with this value increasing upon additional silane modification. This shows the opposite behavior to that known for silica-filled samples, where silanization reduces the 'Payne-Effect' to a certain amount. The concentration of hydroxyl groups, present on the surface of the nanotubes, is not comparable to silica and does not allow the formation of hydrogen-bonds between two adjacent modified tubes, hence the silanization does not reduce the filler-filler interaction.

The direct current (DC) electrical percolation behavior of the nanocomposites is depicted in Figure 8. It is evident from this figure that there is a sharp rise of conductivity when the filler concentration is increased from 1 to 2 phr for the wet mixed samples. This sudden rise in conductivity is an effect of the formation of a continuous network of the carbon nanotubes. The very

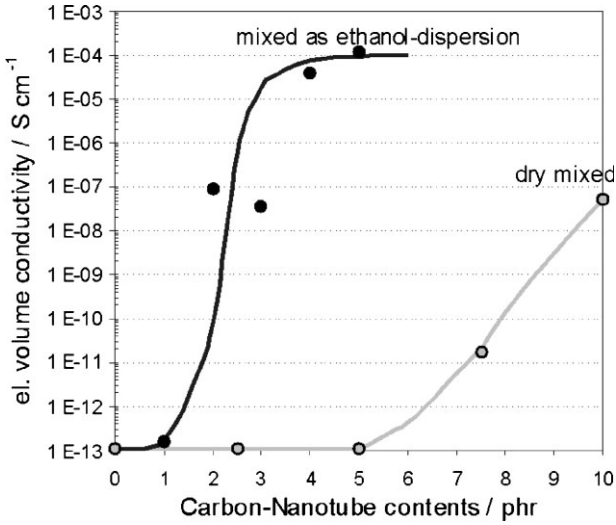

Figure 8.
Dependence of DC electrical conductivity on the CNT content of S-SBR-BR blends. The filled round symbols represent the conductivity of the CNT-filled vulcanizates mixed by wet mixing, while the unfilled round symbols denote the conductivity of the dry-mixed samples.

high aspect ratio of CNTs is mainly responsible for this percolation behavior at very low CNT loadings. In the case of dry mixed vulcanizates, a steady increment of the conductivity can be observed starting at a CNT loading of 5 phr which is significantly higher than in the wet mixed samples. Hence, the dispersion of CNTs is considerably improved when the mixing is done by the ethanol predispersion leading to the formation of the CNT network with a smaller amount of filler.

Conclusion

A novel method for the preparation of solution styrene butadiene rubber (S-SBR) is described with the use of a polar rubber as a vector to transport layered silicate into the non-polar S-SBR matrix.

The effects of both sulfur and peroxide curing on the intercalation and exfoliation process of the layered silicate are studied to find a suitable vulcanization package for acrylonitrile butadiene rubber (NBR). X-ray diffraction and transmission electron microscopy studies showed that proper selection of a curing package leads to excellent dispersion of the layered silicates in intercalated form.

Triethoxysilyl grafted ethylene-propylene-diene-monomer rubber (EPDM), filled with the *in situ* sol-gel silica particles, was found to exhibit excellent physical properties, despite the fact that the fraction of silica fillers in this material is found to be very low. The *in situ* produced sol-gel silica nanoparticles have higher reinforcing efficiency, attributed to the formation of a rubber-silica network.

Concerning the dispersion of carbon nanotubes in styrene butadiene rubber-butadiene rubber blends (S-SBR-BR) we offered a novel method to get rubber nanocomposites at very low loading of carbon-like fillers. The high aspect ratio of the carbon nanotubes enabled the formation of a conductive percolating network in these composites at concentrations below 2% wt. Finally, the 'Payne effect', an indication of the establishment of filler-filler interactions, was observed at very low concentrations of CNTs in the rubber matrix.

In summary, we have depicted several routes to rubber nanocomposites for different industrial applications. It is important to note that all these approaches can be scaled up and realized in commercially available rubber processing equipment. Thus, we suppose that these approaches have the potential to trigger the development of next-generation rubber materials with advanced technical performance.

Acknowledgements: This work has been supported by the German Federal Ministry of Education and Research (BMBF Grant 03X0002E). We also acknowledge Dr. Manfred Klüppel and Juliane Fritzsche (DIK, Hannover, Germany) for their fruitful cooperation.

[1] D. Kang, D. Kim, S. H. Yoon, D. Kim, C. Barry, J. Mead, *Macromol. Mater. Eng.* **2007**, *292*, 329–338.
[2] P. L. Teh, Z. A. Mohd Ishak, A. S. Hashim, J. Karger-Kocsis, U. S. Ishiaku, *Eur. Polym. J.* **2004**, *40*, 2513–2521.
[3] J. Ma, P. Xiang, Y.-W. Mai, L.-Q. Zhang, *Macromol. Rapid. Commun.* **2004**, *25*, 1692–1696.
[4] M. Arroyo, M. A. Lopez-Manchado, B. Herrero, *Polymer* **2003**, *44*, 2447–2453.
[5] S. Sadhu, A. K. Bhowmick, *Rubb. Chem. Technol.* **2003**, *76*, 860–875.
[6] S. Pradhan, F. R. Costa, U. Wagenknecht, D. Jehnichen, A. K. Bhowmick, G. Heinrich, *Eur. Polym. J.* **2008**, *44*, 3122–3132.
[7] V. Thakur, A. Das, R. N. Mahaling, S. Rooj, U. Gohs, U. Wagenknecht, G. Heinrich, *Macromol. Mater. Eng.* **2009**, *294*, 561–569.
[8] Q. W. Yuan, J. E. Mark, *Macromol. Chem. Phys.* **1999**, *200*, 206–220.
[9] A. S. Hashim, B. Azahari, Y. Ikeda, S. Kohjiya, *Rubb. Chem. Technol* **1998**, *71*, 289–299.
[10] J. Yangab, M. Tiana, Q.-X. Jiab, J.-H. Shia, L.-Q. Zhangab, S.-H. Limc, Z.-Z. Yuc, Y.-W. Maic, *Acta Mater.* **2007**, *55*, 6372–6382.
[11] L. Chen, G. Chen, L. Lu, *Adv. Func. Mater.* **2007**, *17*, 898–904.
[12] L. Bokobza, *Polymer* **2007**, *48*, 4907–4920.
[13] M. D. Frogley, D. Ravich, H. D. Wagner, *Comp. Sci. Technol.* **2003**, *63*, 1647–1654.
[14] A. Das, R. Jurk, K. W. Stöckelhuber, G. Heinrich, *J. Macromol. Sci. Chem.* **2008**, *45*, 101–106.
[15] A. Das, R. Jurk, K. W. Stöckelhuber, T. Engelhardt, J. Fritzsche, M. Klüppel, G. Heinrich, *J. Macromol. Sci. Chem.* **2008**, *45*, 144–150.

[16] A. Das, R. Jurk, K. W. Stöckelhuber, G. Heinrich, *Macromol. Mater. Eng.* **2008**, *293*, 479–490.
[17] A. Das, R. Jurk, K. W. Stöckelhuber, G. Heinrich, *eXPRESS Polym. Lett.* **2008**, *1*, 717–723.
[18] J. Fritzsche, A. Das, R. Jurk, K. W. Stöckelhuber, G. Heinrich, M. Klüppel, *eXPRESS Polym. Lett.* **2008**, *2*, 373–381.
[19] M. Moniruuzzaman, K. I. Winey, *Macromolecules* **2006**, *39*, 5194–5205.
[20] A. Das, K. W. Stöckelhuber, R. Jurk, M. Saphiannikova, J. Fritzsche, H. Lorenz, M. Klüppel, G. Heinrich, *Polymer* **2008**, *49*, 5278–5283.
[21] A. Das, K. W. Stöckelhuber, R. Jurk, J. Fritzsche, M. Klüppel, G. Heinrich, *Carbon* **2009**, *47*, 3313–3321.
[22] Y. Ma, Q. F. Li, L. Q. Zhang, Y. P. Wu, *Polym. J.* **2007**, *39*, 48–54.
[23] G. Heinrich, M. Klüppel, *Adv. Polym. Sci.* **2002**, *160*, 1–44.

